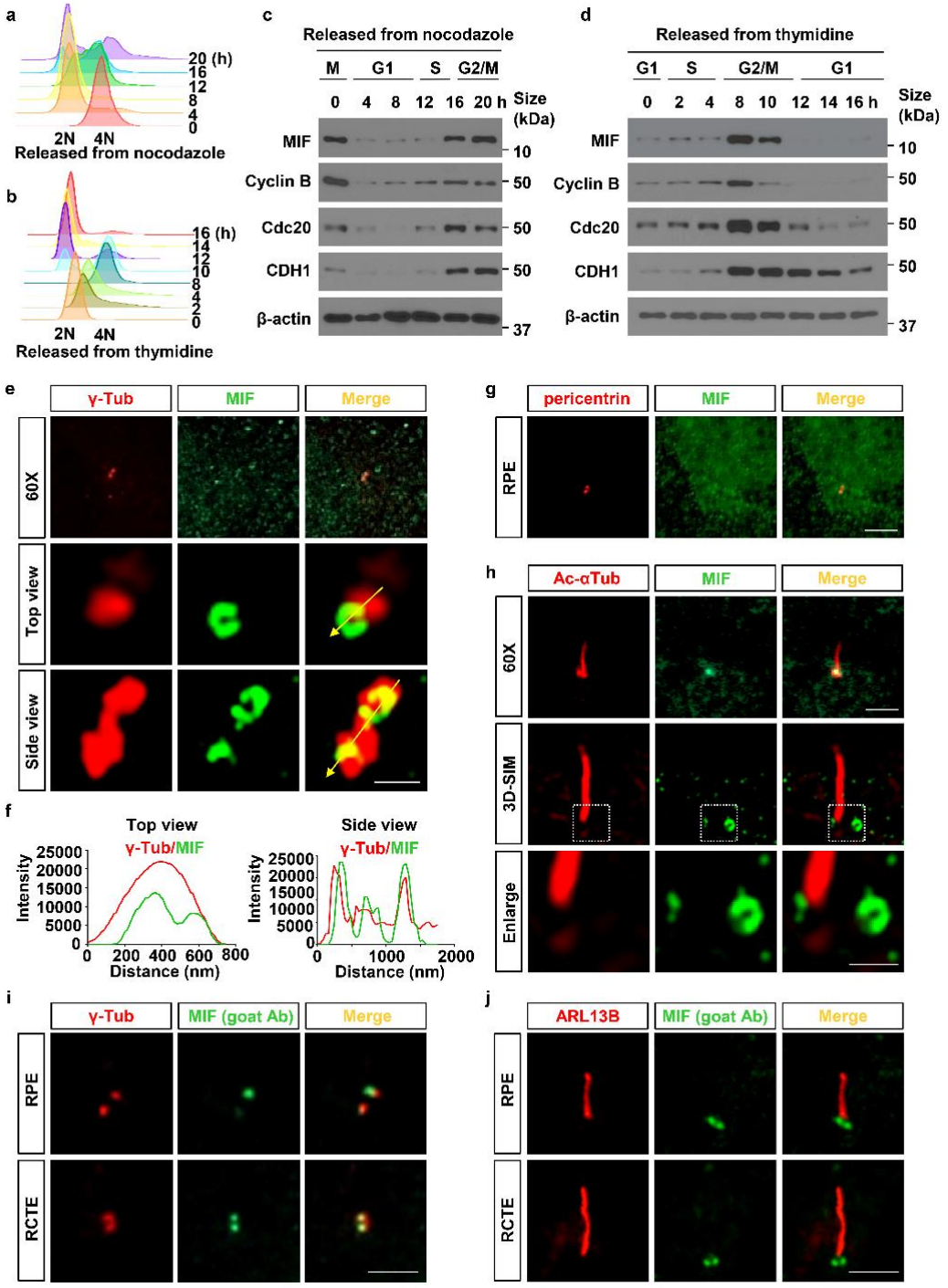
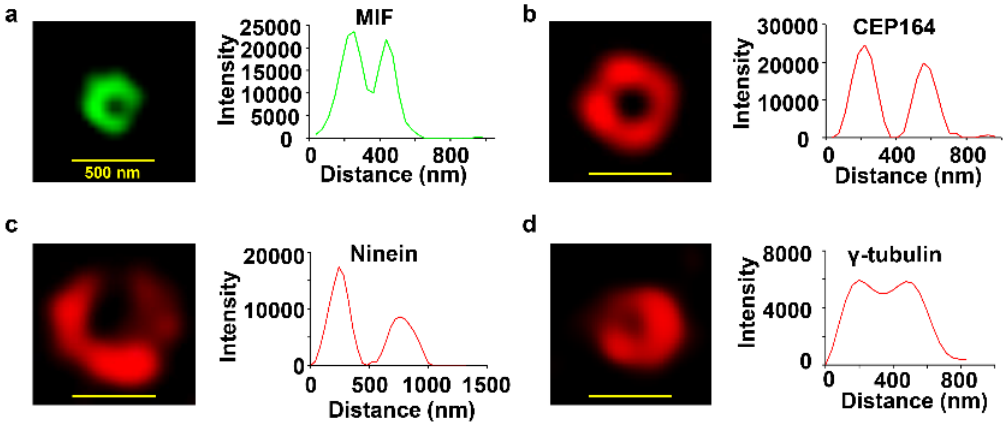
Supplementary Figures and Figure legends



Supplementary Figure 1. The levels of MIF protein fluctuate throughout cell cycle and MIF is located at cilia base body. a, **b** FACS analysis was used to estimate the cell-cycle profiles in thymidine-nocodazole (**a**) and double thymidine (**b**) treated cells by measuring the DNA contents in those cells with propidium iodide staining. **c**, **d** Western blot analysis of whole cell lysates derived from Hela cells synchronized in M phase by thymidine-nocodazole (**c**) and in late G1/S phase by double thymidine treatment (**d**) following by releasing back into the cell cycle. **e**

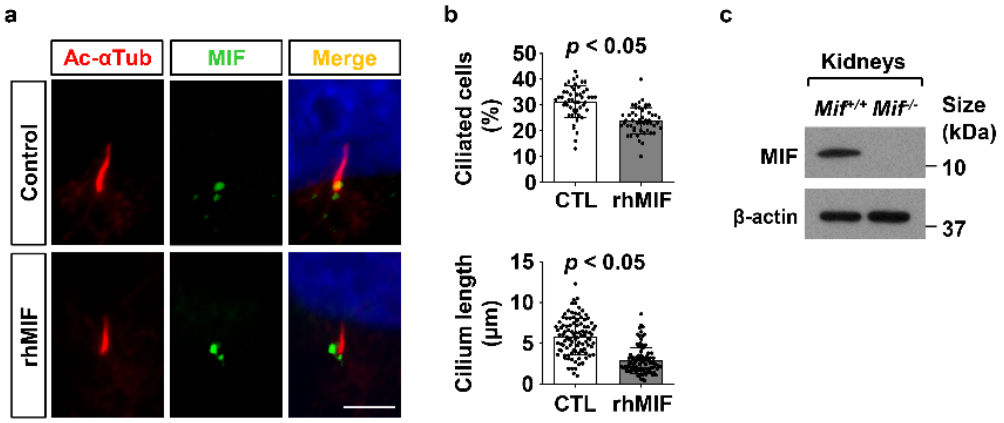
Representative images of RPE cells stained with MIF (green) antibody and co-stained with γ-tubulin (γ-Tub) (red), which were visualized under 2D microscope and three-dimensional structured illumination microscopy (3D-SIM). Scale bars, 5 μm (*top panels*) and 500 nm (*middle and bottom panels* of 3D images)**. f** The intensity plots of the rings in 3D images (**e**) from top and side views. **g** Representative images of RPE cells stained with MIF (green) antibody and co-stained with pericentrin (red). Scale bars, 5 μm. **h** Representative images of RPE cells stained with MIF (green) antibody and co-stained with acetylated α-tubulin (Ac-α-Tub) (red), which were visualized under 2D microscope and 3D-SIM microscopy. Scale bars, 5 μm (*top panels*) and 500 nm (*middle panels* of 3D images). **i**, **j** Representative images of RPE and RCTE cells stained with a second MIF antibody (green) and co-stained with γ-tubulin (red) (**i**) or ARL13B (red) antibody (**j**). Scale bars, 5 μm.



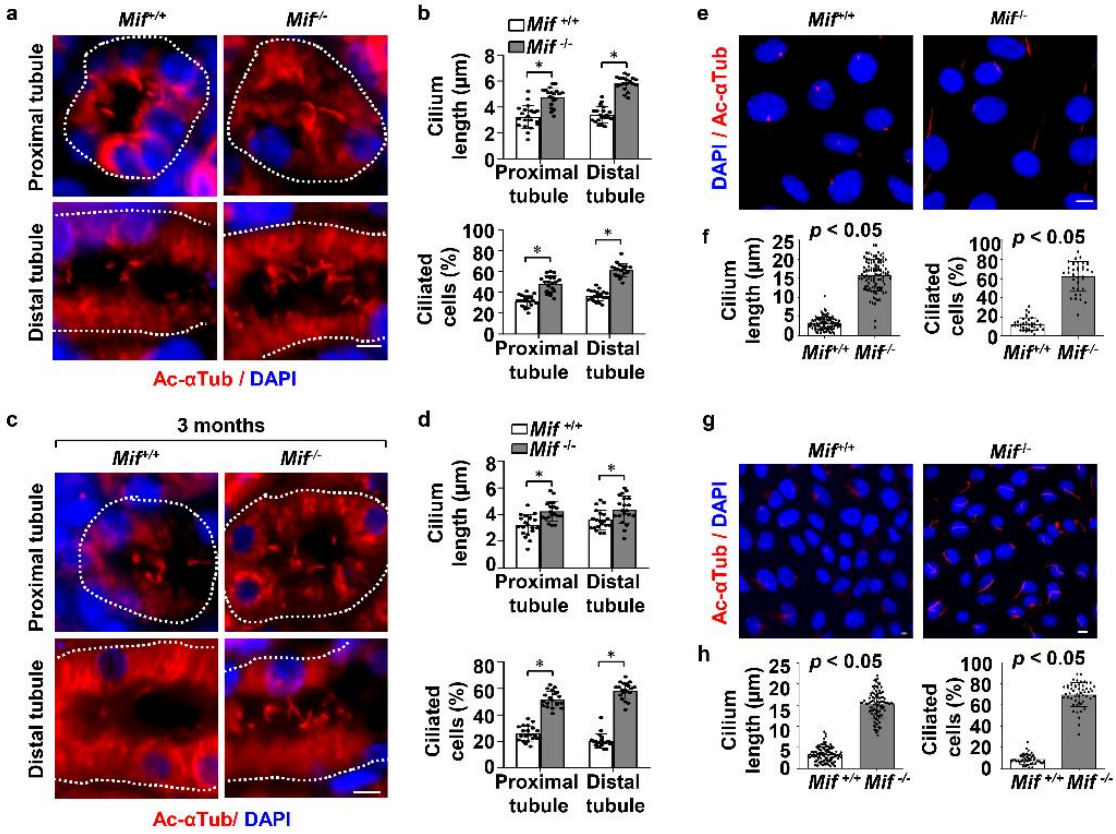
e

Protein	Localization	Diameter(nm)	M(kDa)
MIF	Proximal End of centrioles	307±5.9	13
γ-tubulin	Intermediate PCM	401.3±14.2	51
Ninein	Subdistal appendages	590±13.2	244
CEP164	Distal appendages	409.1±9.4	164

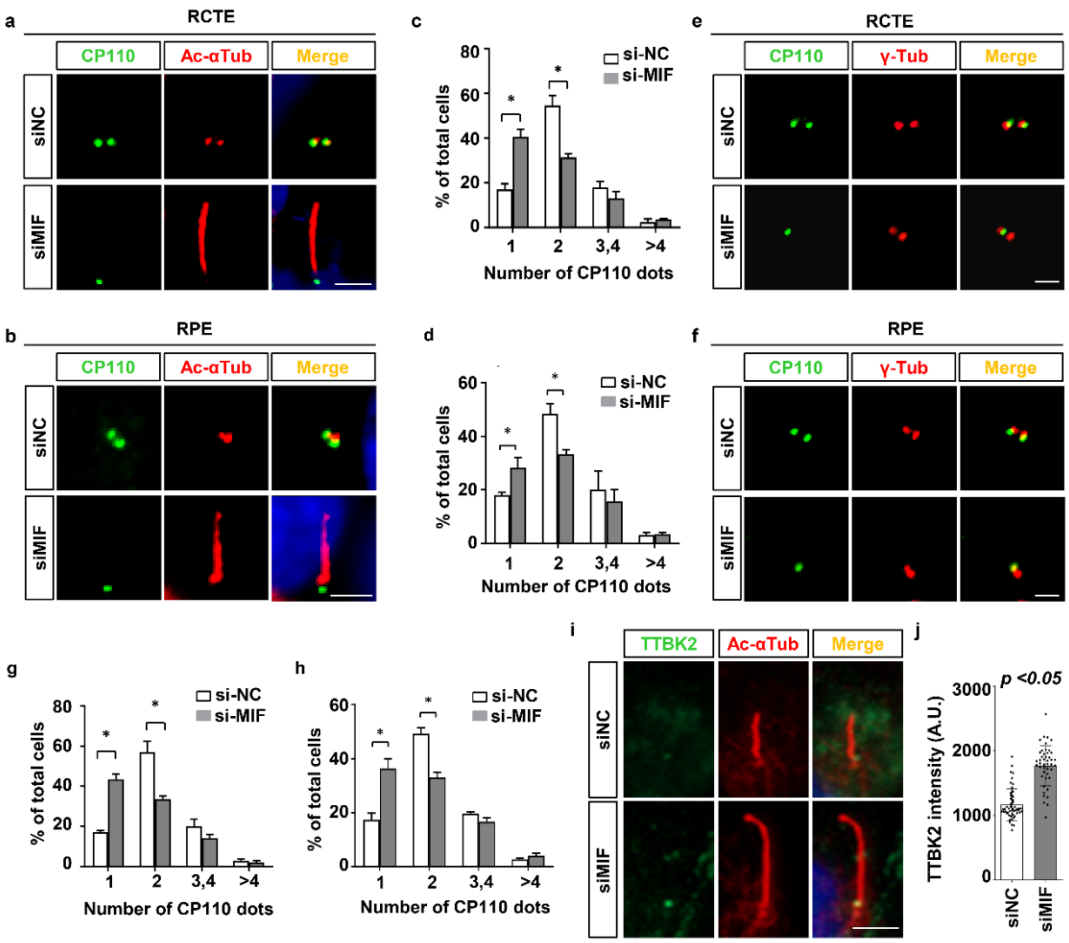
Supplementary Figure 2. Distinct radial distances of centrosomal proteins from centriole walls. a-d 3D-SIM views (*left*) and radial distances (*right*) of centrosomal proteins, MIF, CEP164, Ninein, and γ-tubulin, at centrioles in RCTE cells. Scale bars, 500 nm. **e** The diameters of ring-like structures formed by centrosomal proteins, MIF, CEP164, Ninein, and γ-tubulin around centrioles were determined by the measurement of distances between intensity maxima (mean ± sd).



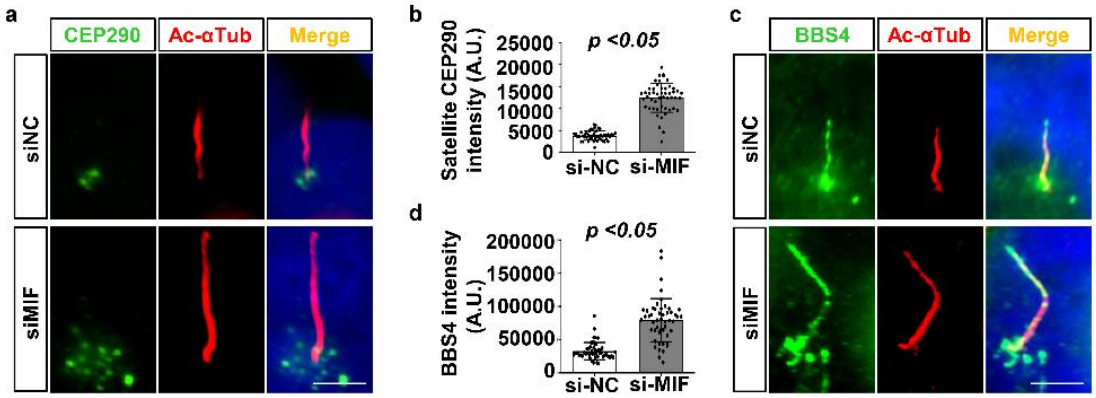
Supplementary Figure 3. Treatment with rhMIF inhibited cilia assembly and elongation in RCTE cells. a Representative images of RCTE cells treated with rhMIF (10 ng/ml) and vehicle (control) plus serum free for 24h, and then stained with MIF (green) and acetyl-α-tubulin (red) antibodies and co-stained with DAPI (blue) ($n = 3$). Scale bars, 5 μm. **b** Treatment with rhMIF decreased the percentage of ciliated cells (top) and cilia length (bottom). The ciliated cell percentages of about 50 views was analyzed in each group; The cilia lengths of about 100 cells was analyzed in each group. **c** Western blot analysis of Mif in kidneys from wild type and *Mif* knockout mice ($n = 5$). All data are represented as the mean value ± s.d. Significant differences were identified by student's *t*-test.



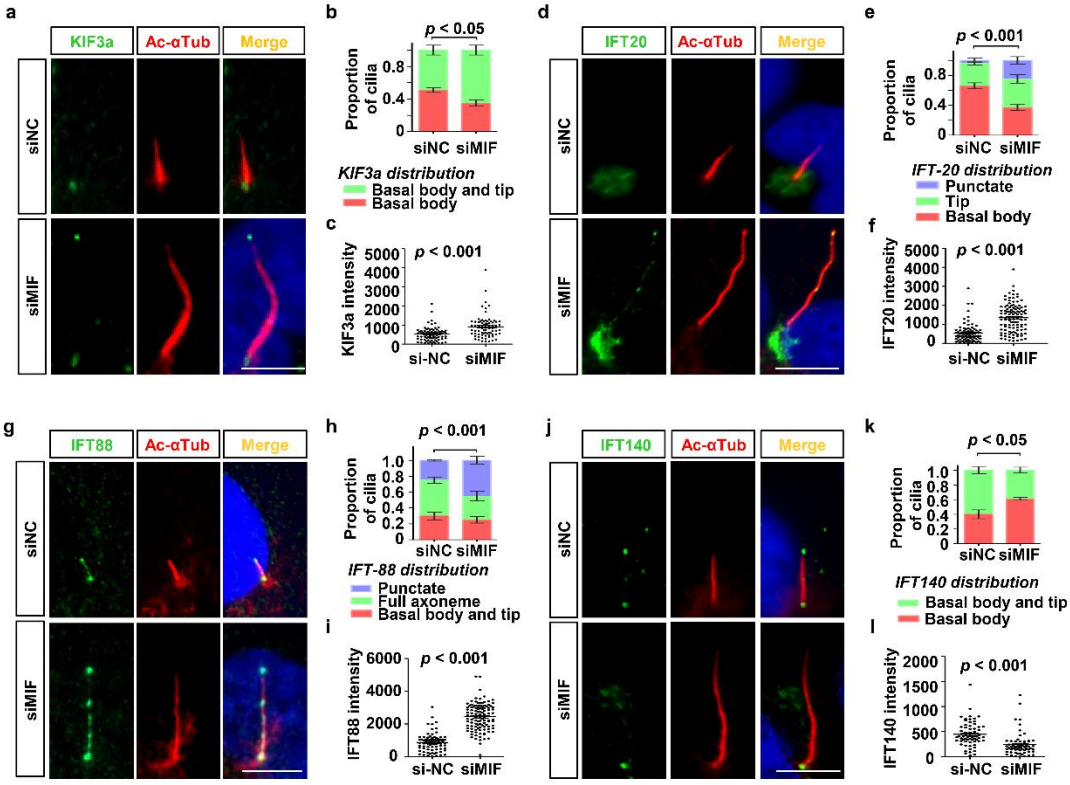
Supplementary Figure 4. Knockout of MIF facilitated ciliogenesis in primary renal tubule cells and in the lumens of renal tubules. a Representative images of kidney sections from 21 days old *Mif* $^{+/+}$ and *Mif* $^{-/-}$ mice (n = 5 mice for each group) stained with acetyl-α-tubulin (red) and DAPI (blue). White dashed lines represent the border of each renal tubule. Scale bars, 5 μm. **b** Knockout of Mif in kidneys (**a**) increased cilia length (top) and the percentage of ciliated cells (bottom) in the lumens of renal tubules compared to the controls, which were quantified and plotted from three independent experiments. *p <0.05. **c** Representative images of kidney sections from 3 months old *Mif* $^{+/+}$ and *Mif* $^{-/-}$ mice (n = 5 mice for each group) stained with acetyl-α-tubulin (red) and DAPI (blue). White dashed lines represent the border of each renal tubule. Scale bars, 5 μm. **d** Knockout of Mif in kidneys (**c**) increased cilia length (top) and the percentage of ciliated cells (bottom) in the lumens of renal tubules compared to the controls, which were quantified and plotted from three independent experiments. *p <0.05. **e** Representative images of primary renal tubule cells isolated form 21 days old *Mif* $^{+/+}$ and *Mif* $^{-/-}$ kidneys (n = 5 mouse kidneys for each group) and stained with acetyl-α-tubulin (red) and DAPI (blue). Scale bars, 5 μm. **f** Knockout of Mif in primary renal tubule cells (**e**) increased cilia length (left) and the percentage of ciliated cells (right) compared to the controls, which were quantified and plotted from three independent experiments. **g** Representative images of primary renal tubular cells isolated form 3 months old *Mif* $^{+/+}$ and *Mif* $^{-/-}$ kidneys (n = 5 mouse kidneys for each group) and stained with acetyl-α-tubulin (red) and DAPI (blue). Scale bars, 5 μm. **h** Knockout of Mif in primary renal tubular cells (**g**) increased cilia length (left) and the percentage of ciliated cells (right) compared to the controls, which were quantified and plotted from three independent experiments. All data are represented as the mean value ± s.d. Significant differences were identified by student's *t*-test.



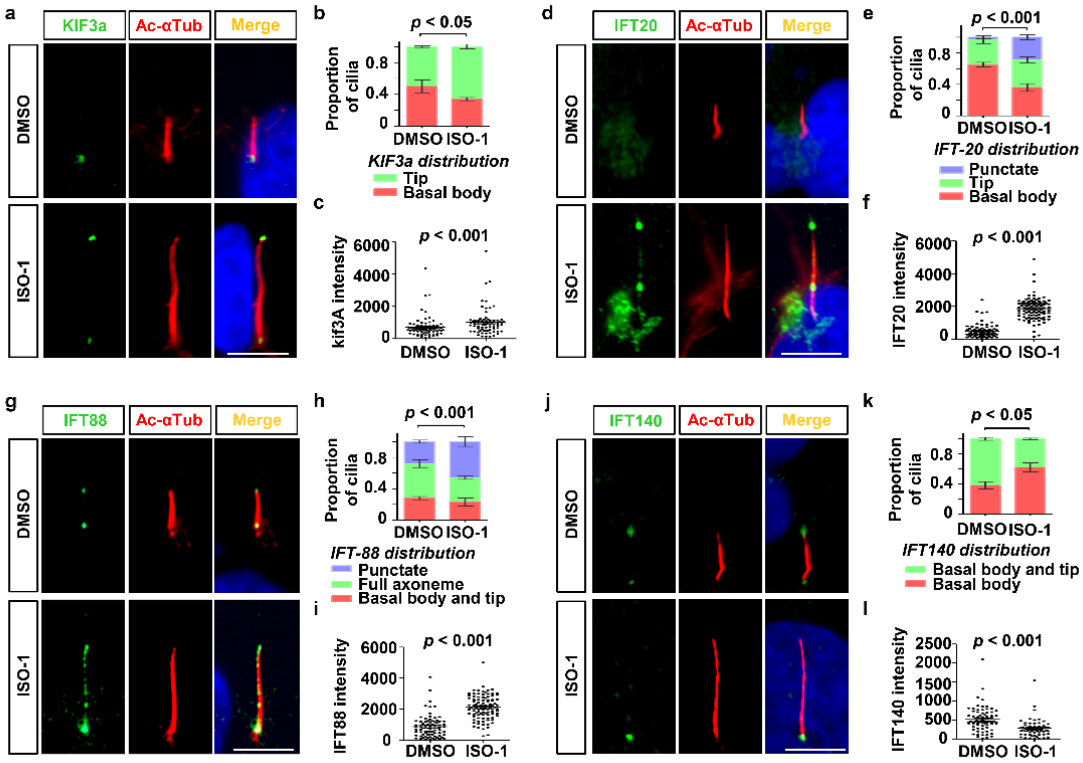
Supplementary Figure 5. Depletion of MIF increases the removal of CP110 from mother centriole and the recruitment of TTBK2 to basal body. a, **b** Representative images of RCTE (**a**) and RPE (**b**) cells transfected with MIF and control siRNAs and then stained with CP110 (green) and acetyl-α-tubulin (red) antibodies and co-stained with DAPI (blue). Scale bars, 5 μm. **c**, **d** Quantification of the percentage of cells with the indicated numbers of CP110 dots at centrioles in MIF knockdown RCTE (**c**) and RPE (**d**) cells from three independent experiments. *p <0.05. **e, f** Representative images of RCTE (**e**) and RPE (**f**) cells transfected with MIF and control siRNAs and then stained with CP110 (green) and γ-tubulin (red) antibodies. Scale bars, 5 μm. **g**, **h** Quantification of the percentage of cells with the indicated numbers of CP110 dots at centrioles in MIF knockdown RCTE (**g**) and RPE (**h**) cells from three independent experiments. *p <0.05. **i** Representative images of RCTE cells transfected with MIF and control siRNAs and then stained with TTBK2 (green) and acetyl-α-tubulin (red) antibodies and co-stained with DAPI (blue). Scale bars, 5 μm. **j** Quantification of the intensity of TTBK2 at basal body in RCTE cells from three independent experiments. About 30 cells was analyzed in each group (**c**, **d**, **g**, **h**). Statistics were performed using multiple *t*-test (**c**, **d**, **g**, **h**). Statistics were performed using student's *t*-test (**j**).



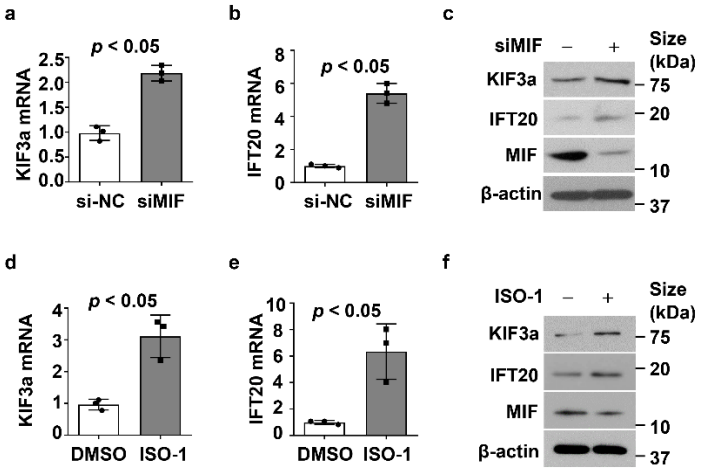
Supplementary Figure 6. Depletion of MIF increases the accumulation of CEP290 and BBS4 at centriolar satellites. a Representative images of RCTE cells transfected with MIF and control siRNAs and then stained with CEP290 (green) and acetyl-α-tubulin (red) antibodies and co-stained with DAPI (blue). Scale bars, 5 μm. **b** Quantification of the intensity of CEP290 at centriolar satellites in RCTE cells from three independent experiments. **c** Representative images of RCTE cells transfected with MIF and control siRNAs for 48h and serum starved for 24h, and then stained with BBS4 (green) and acetyl-α-tubulin (red) antibodies and co-stained with DAPI (blue). Scale bars, 5 μm. **d** Quantification of the intensity of BBS4 at centriolar satellites in RCTE cells from three independent experiments. About 50 cells was analyzed in each group (**b**, **d**). All data are represented as the mean value ± s.d. Significant differences were identified by student's *t*-test.



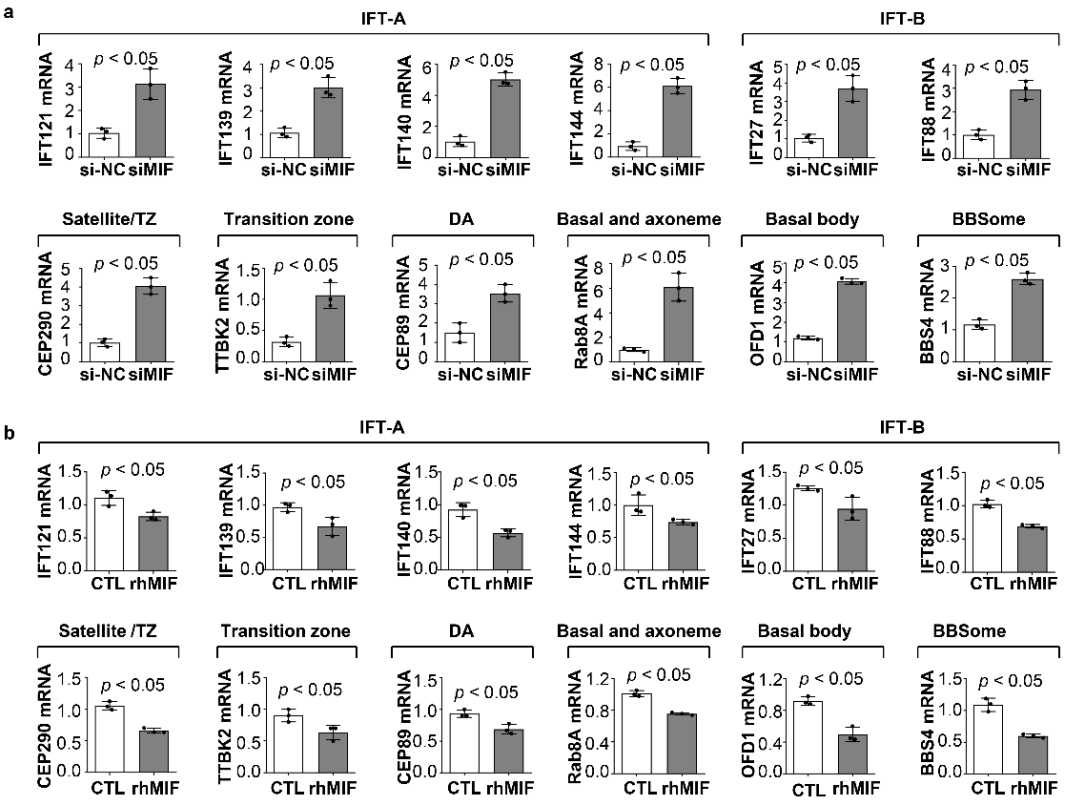
Supplementary Figure 7. **Knockdown of MIF affects the trafficking of KIF3a and IFT particles, including IFT20, IFT88 and IFT140. a** Representative image of RCTE cells transfected with MIF and control siRNAs for 48h and serum starved for 24h, then stained with KIF3a (green) and acetyl-α-tubulin (red) antibodies and co-stained with DAPI (blue). Scale bars, 5 μm. **b** Stacked bar graph represented KIF3a distribution at primary cilia in RCTE cells transfected with MIF and control siRNAs. **c** Quantification of the intensity of KIF3a signals in RCTE cells transfected with MIF and control siRNAs. **d** Representative images of RCTE cells transfected with MIF and control siRNAs for 48h and then serum starved for 24h, and stained with IFT20 (green) and acetyl-α-tubulin (red) antibodies and co-stained with DAPI (blue). Scale bars, 5 μm. **e** Stacked bar graph represented IFT20 distribution at primary cilia in RCTE cells transfected with MIF and control siRNAs. **f** Quantification of the intensity of IFT20 signals in RCTE cells transfected with MIF and control siRNAs. **g** Representative images of RCTE cells transfected with MIF and control siRNAs for 48h and then serum starved for 24h, and stained with IFT88 (green) and acetyl-α-tubulin (red) antibodies and co-stained with DAPI (blue). Scale bars, 5 μm. **h** Stacked bar graph represented IFT88 distribution at primary cilia in RCTE cells transfected with MIF and control siRNAs. **i** Quantification of the intensity of IFT88 signals in RCTE cells transfected with MIF and control siRNAs. **j** Representative images of RCTE cells transfected with MIF and control siRNAs for 48h and then serum starved for 24h, and stained with IFT140 (green) and acetyl-α-tubulin (red) antibodies and co-stained with DAPI (blue). Scale bars, 5 μm. **k** Stacked bar graph represented IFT140 distribution at primary cilia in RCTE cells transfected with MIF and control siRNAs. **l** Quantification of the intensity of IFT140 signals in RCTE cells transfected with MIF and control siRNAs. $n = 3$ biologically independent experiments. About 100 cells was analyzed in each group. Statistics were performed using one-sided one-way ANOVA followed by post hoc LSD test (**b**, **e**, **h**, **k**). Statistics were performed using student's *t*-test (**c**, **f**, **i**, **l**).



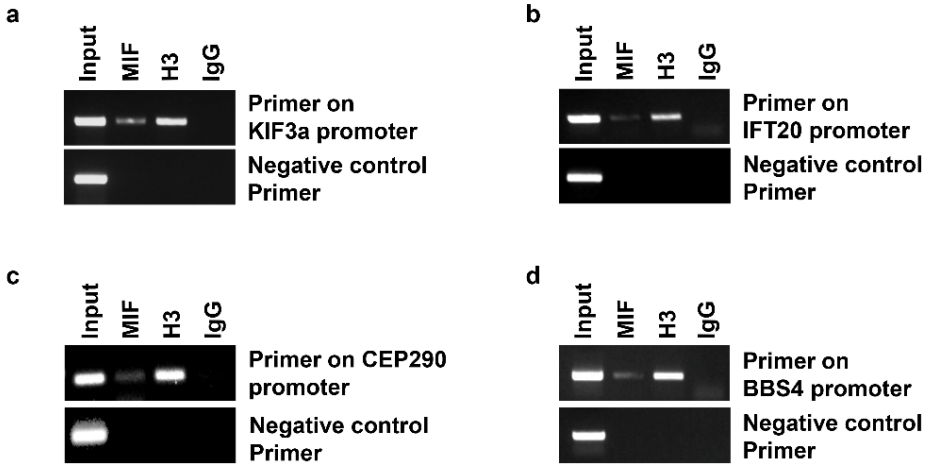
Supplementary Figure 8. Inhibition of MIF affects the trafficking of KIF3a and IFT particles, including IFT20, IFT88 and IFT140. a Representative images of RCTE cells treated with ISO-1 and DMSO, then serum starved for 24h and stained with KIF3a (green) and acetyl-α-tubulin (red) antibodies and co-stained with DAPI (blue). Scale bars, 5 μm. **b** Stacked bar graph represented KIF3a distribution at primary cilia in RCTE cells treated with ISO-1 and DMSO. **c** Quantification of the intensity of KIF3a signals in RCTE cells treated with ISO-1 and DMSO. **d** Representative images of RCTE cells treated with ISO-1 and DMSO, then serum starved for 24h and stained with IFT20 (green) and acetyl-α-tubulin (red) antibodies and co-stained with DAPI (blue). Scale bars, 5 μm. **e** Stacked bar graph represented IFT20 distribution at primary cilia in RCTE cells treated with ISO-1 and DMSO. **f** Quantification of the intensity of IFT20 signals in RCTE cells treated with ISO-1 and DMSO. **g** Representative images of RCTE cells treated with ISO-1 and DMSO, then serum starved for 24h and stained with IFT88 (green) and acetyl-α-tubulin (red) antibodies and co-stained with DAPI (blue). Scale bars, 5 μm. **h** Stacked bar graph represented IFT88 distribution at primary cilia in RCTE cells treated with ISO-1 and DMSO. **i** Quantification of the intensity of IFT88 signals in RCTE cells treated with ISO-1 and DMSO. **j** Representative images of RCTE cells treated with ISO-1 and DMSO, then serum starved for 24h and stained with IFT140 (green) and acetyl-α-tubulin (red) antibodies and co-stained with DAPI (blue). Scale bars, 5 μm. **k** Stacked bar graph represented IFT140 distribution at primary cilia in RCTE cells treated with ISO-1 and DMSO. **l** Quantification of the intensity of IFT140 signals in RCTE cells treated with ISO-1 and DMSO. $n = 3$ biologically independent experiments. About 100 cells was analyzed in each group. Statistics were performed using one-sided one-way ANOVA followed by post hoc LSD test (**b**, **e**, **h**, **k**). Statistics were performed using student's *t*-test (**c**, **f**, **i**, **l**).



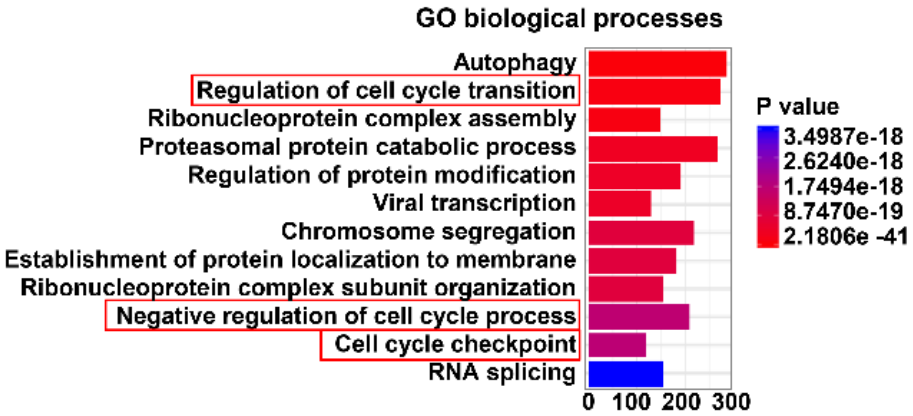
Supplementary Figure 9. **Knockdown and inhibition of MIF increased the mRNA and protein levels of KIF3a and IFT20 in RCTE cells. a-c** Knockdown of MIF with siRNA increased the expression of KIF3a and IFT20 in RCTE cells compared to that in the control cells as examined with RT-PCR (**a** and **b**) and Western blot (**c**) analysis. **d-f** Inhibition of MIF with ISO-1 increased the expression of KIF3a and IFT20 in RCTE cells compared to that in the control cells as examined with RT-PCR (**d** and **e**) and Western blot (**f**) analysis. $n = 3$ biologically independent experiments. All data are represented as the mean value ± s.d. Significant differences were identified by student's *t*-test.



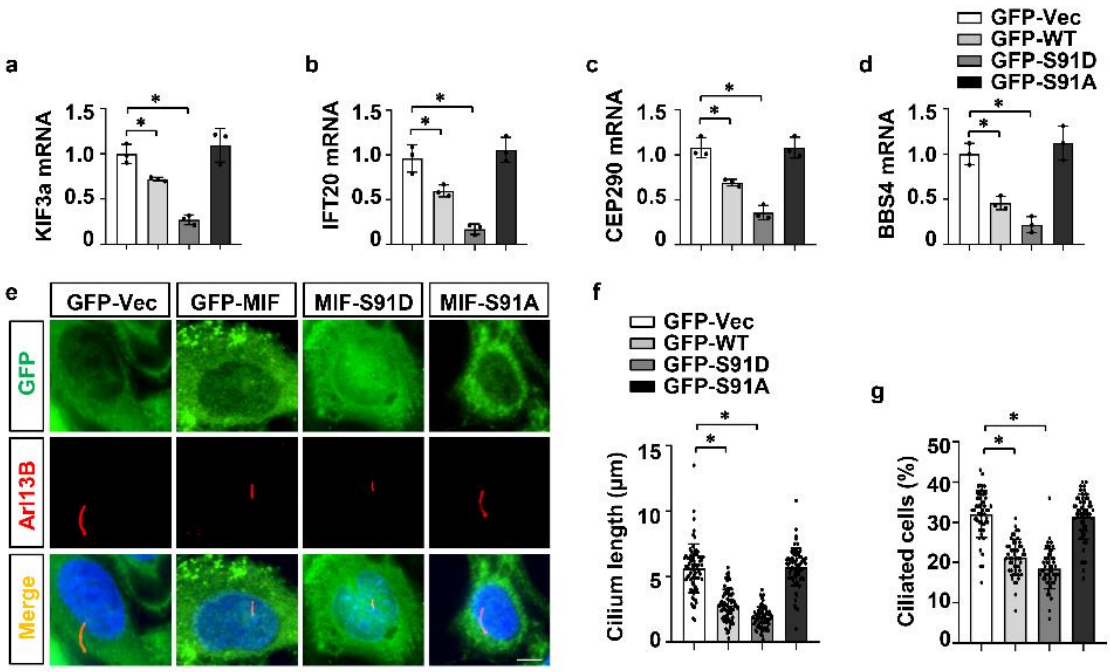
Supplementary Figure 10. **MIF regulates the transcription of ciliary genes. a** qRT-PCR analysis of the expression of ciliary genes, including IFT A particles (IFT121, IFT139, IFT140, IFT144), IFT B particles (IFT27, IFT88), centriolar satellite/ transition zone protein (CEP290), transition zone protein (TTBK2), distal appendage protein (CEP89), basal body and axoneme protein (Rab8a), basal body protein (OFD1) and BBSome protein (BBS4) in RCTE cells transfected with MIF and control siRNAs. **b** qRT-PCR analysis of the expression of ciliary genes, including IFT121, IFT139, IFT140, IFT144, IFT27, IFT88, CEP290, TTBK2, CEP89, Rab8a, OFD1 and BBS4 in RCTE cells treated with rhMIF and vehicle (control). n = 3 biologically independent experiments. All data are represented as the mean value ± s.d. Significant differences were identified by student's *t*-test.



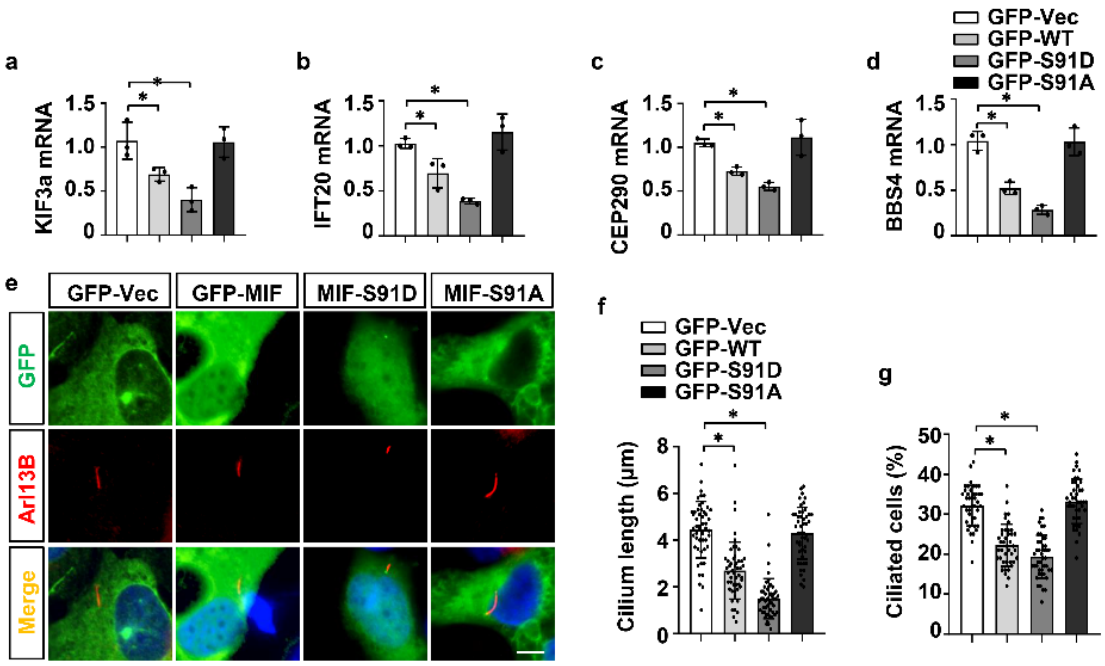
Supplementary Figure 11. **MIF directly binds to the promoter of ciliary genes, including *IFT20, KIF3a, CEP290* and *BBS4*. a-d** ChIP assay was performed with anti-MIF antibody or IgG (control) to detect the binding of MIF on the promoters of *KIF3a* (**a**), *IFT20* (**b**)*, CEP290* (**c**) and *BBS4* (**d**) in RCTE cells. Anti-H3 antibody was used as a positive control. Negative control (NC) primers were located about 2000 bp upstream of the transcription start site (TSS) of tested genes.



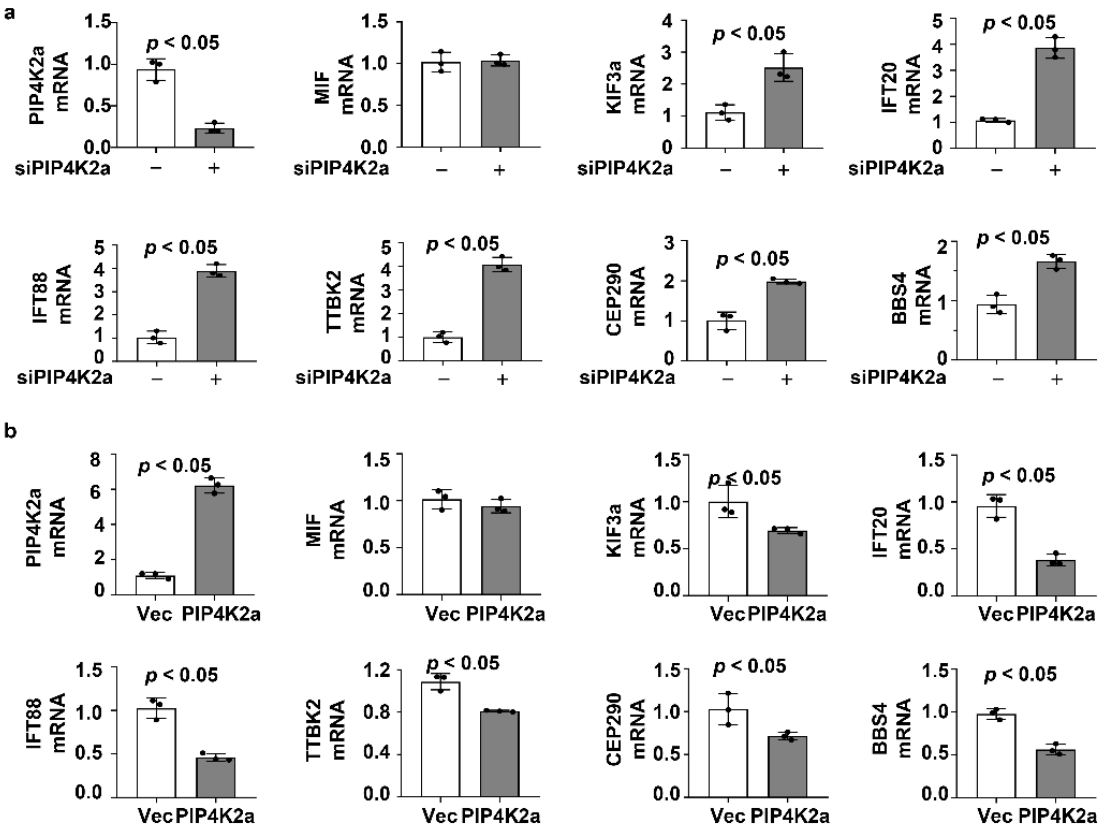
Supplementary Figure 12. GO biological processes analysis of MIF target genes. The analysis of biological processes categories identified potential MIF target genes related to signaling pathways of autophagy, cell cycle transition and cell cycle checkpoint, etc.



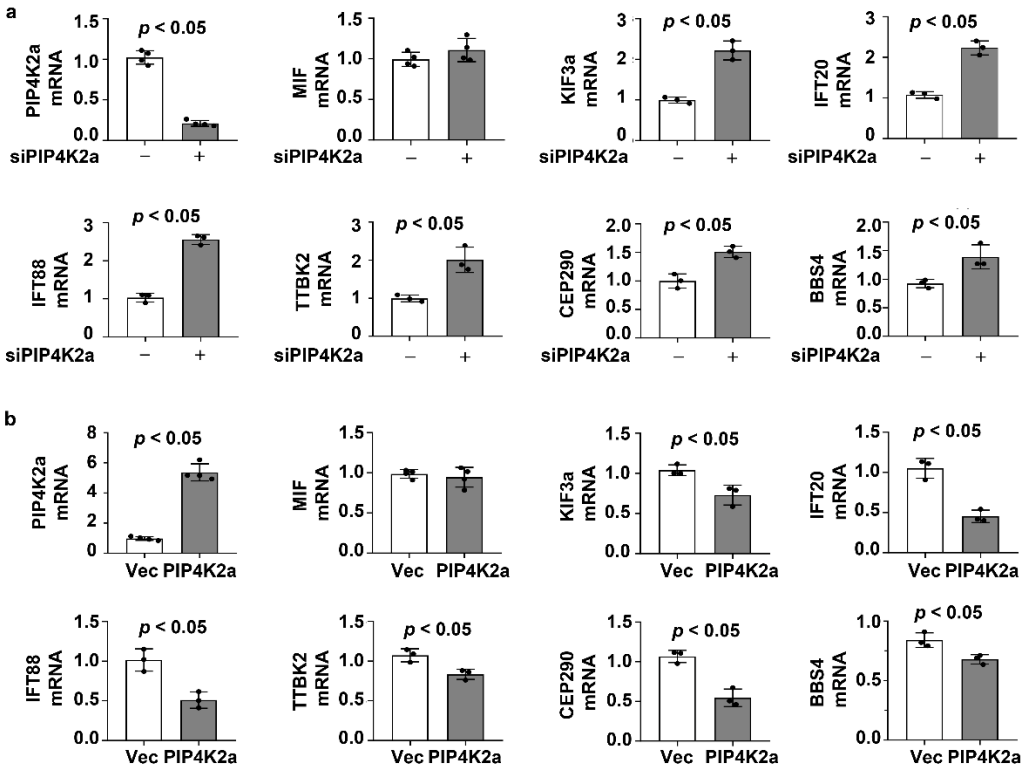
Supplementary Figure 13. **Overexpression of GFP tagged wild type MIF and mutant MIF-S91D decreased the expression of cilia related genes and ciliogenesis in RCTE cells. a-d** qRT-PCR analysis of the expression of KIF3a (**a)**, IFT20 (**b**), CEP290 (**c**) and BBS4 (**d**) in RCTE cells transfected with GFP-Vector, GFP tagged wild type MIF, GFP tagged mutant MIF-S91D and MIF-S91A plasmids, respectively. **e** Representative images of RCTE cells transfected with GFP-Vector, GFP tagged wild type MIF, GFP tagged MIFS91D or GFP-MIF-S91A plasmids, respectively, and stained with GFP (green) and ARL13B (red) antibodies and co-stained with DAPI (blue). Scale bars, 5 μm. **f**, **g** Statistical analysis of cilium length (**f**) and the percentage of ciliated cells (**g**) in each group of RCTE cells from (**e**). $n = 3$ biologically independent experiments. The cilia lengths of about 100 cells was analyzed in each group; The ciliated cell percentages of about 50 views was analyzed in each group. All data are represented as the mean value ± s.d. Significant differences were identified by student's *t*-test. **p* <0.05.



Supplementary Figure 14. Overexpression of GFP tagged wild type MIF and mutant MIF-S91D decreased the expression of cilia related genes and ciliogenesis in RPE cells. a-d qRT-PCR analysis of the expression of KIF3a (**a**), IFT20 (**b**), CEP290 (**c**) and BBS4 (**d**) in RPE cells transfected with GFP-Vector, GFP tagged wild type MIF, GFP tagged mutant MIF-S91D and MIF-S91A plasmids, respectively. **e** Representative images of RPE cells transfected with GFP-Vector, GFP tagged wild type MIF, GFP tagged MIFS91D or GFP-MIF-S91A plasmids, respectively, and stained with GFP (green) and ARL13B (red) antibodies and co-stained with DAPI (blue). Scale bars, 5 μm. **f**, **g** Statistical analysis of cilium length (**f**) and the percentage of ciliated cells (**g**) in each group of RPE cells from (**e**). $n = 3$ biologically independent experiments. The cilia lengths of about 100 cells was analyzed in each group; The ciliated cell percentages of about 50 views was analyzed in each group. All data are represented as the mean value ± s.d. Significant differences were identified by student's *t*-test. **p* <0.05.



Supplementary Figure 15. Knockdown or overexpression of PIP4K2a affects the transcription of ciliary genes in RCTE cells. a qRT-PCR assay was performed to detect the expression of PIP4K2a, MIF, KIF3a, IFT20, IFT88, TTBK2, CEP290 and BBS4 in RCTE cells transfected with PIP4K2a and control siRNAs. **b** qRT-PCR assay was performed to detect the expression of PIP4K2a, MIF, KIF3a, IFT20, IFT88, TTBK2, CEP290 and BBS4 in RCTE cells transfected with GFP-vector and GFP tagged PIP4K2a plasmids. $n = 3$ biologically independent experiments. All data are represented as the mean value ± s.d. Significant differences were identified by student's *t*-test. *p <0.05.

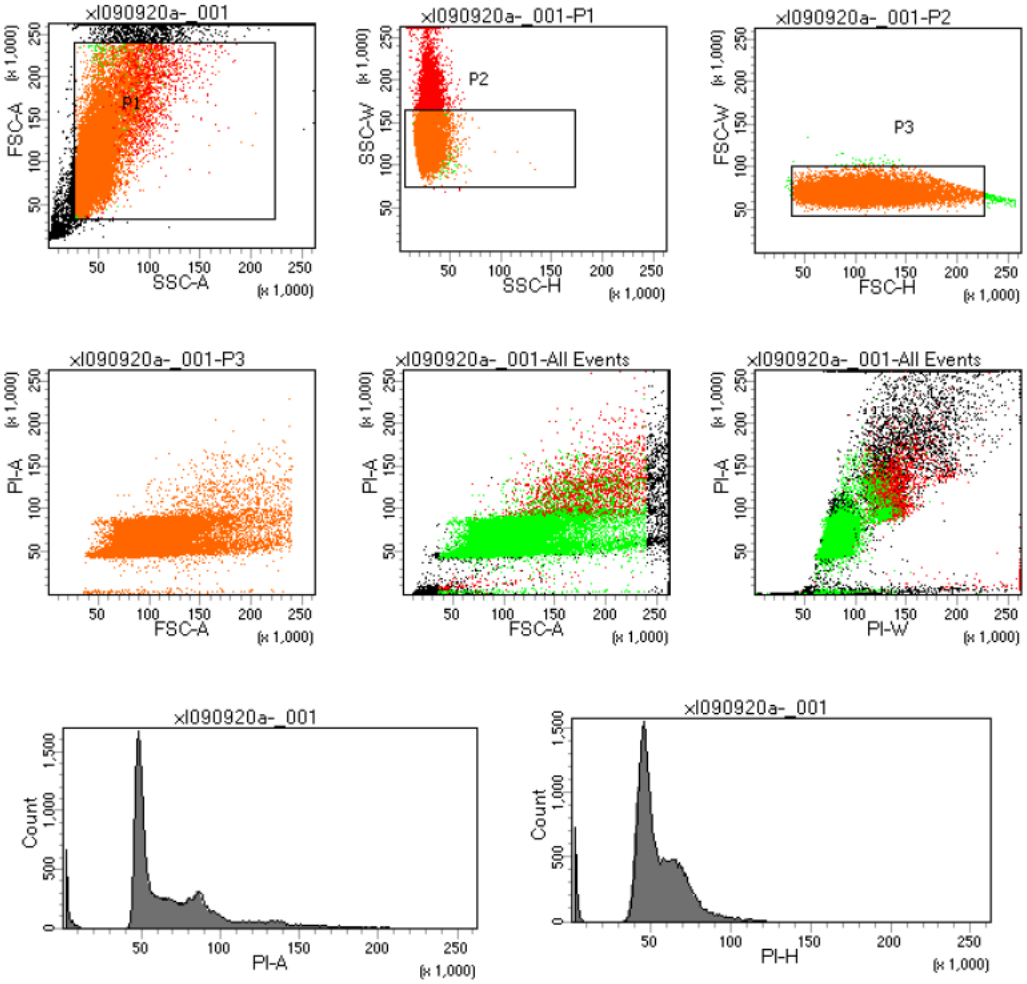


Supplementary Figure 16. Knockdown or overexpression of PIP4K2a affects the transcription of ciliary genes in RPE cells. a qRT-PCR assay was performed to detect the expression of PIP4K2a, MIF, KIF3a, IFT20, IFT88, TTBK2, CEP290 and BBS4 in RPE cells transfected with PIP4K2a and control siRNAs. **b** qRT-PCR assay was performed to detect the expression of PIP4K2a, MIF, KIF3a, IFT20, IFT88, TTBK2, CEP290 and BBS4 in RPE cells transfected with GFP-vector and GFP tagged PIP4K2a plasmids. $n = 3$ or 4 biologically independent experiments. All data are represented as the mean value ± s.d. Significant differences were identified by student's *t*-test. *p <0.05.

Supplementary Table 1. Primers used for quantitative real time PCR and ChIP assay.

Gene name	Forward (5'- 3')	Reverse (5'- 3')
MIF	AGCAGCTGGCGCAGGCCAC	CTCGCTGGAGCCGCCGAAGG
IFT20	AGGCAGGGCTGCATTTTGAT	CAAGCTCAATTAGACCACCAACA
IFT88	CAGTGACAGTGGCCAGAACA	ATCTGTCCCAGGCAAAGCTC
KIF3a	AAAGCGGAGGGTGATACAAG	AACTCCCACATCAGGTCTTTC
BBS4	AAGCAGTGGAGTTCTCACCA	GGCCTTGTAGTTGGTAGGGT
Rab8a	ACATCACCAACGAGAAGTCC	TTTTCTCCCCGTTCCTTGG
IFT121	CATTCAAGGCACAAGGGATC	GGTAGGCTCGACAATTAAGGG
IFT122	CAGTGCCTCGATATAGCTCAAG	AACGCTGGAAGTGGTAGAAC
IFT27	TTCCAGAAAAGCTACACCCTG	ACTCTCCCACAATTTATCCAGC
TTBK2	AGATTTATTGGCTGTGGGAGG	GACTCCAAAATCTGTCTACCCAG
IFT139	GAGACAAAGGGTGGGAGTGA	ACCCTCCAGTAACCTCATGC
IFT140	ATGGACACAGTGACCGTCTT	TCTGGTCCCAGAAGTGGTTC
IFT144	CACTTGTGGATGTTGGAATGC	CATGTTGCTAGGCTCTGATCTC
CEP290	AGACAAATGGCCTGGGATCA	GGCAAACTAGGGTCAGGGAT
CEP89	GTGCCAAATGCCAAGAACTC	GTCAGCTTCTCCATCAACTCC
OFD1	GGGATATGTCTCATGTGGACG	TCTCTGCCTTCGTTCTTTCAC
GAPDH	TGCACCACCAACTGCTTAGC	GGCATGGACTGTGGTCATGAG
CEP290 promoter	GACTGCTCCCCTCAATTCC	TTTTCCTAAGCCATCCCCTG
CEP290 promoter-NC	AAAGTCTGTCCATATATTTTAGGTTGAG	TTTGATTCCTGATCCTTACTCTGG
IFT20 promoter	AGTTTCCACTGATAGCCACAG	CATTAGCTTCGTTGCGTGAG
IFT20 promoter-NC	CCTCCGCTACCTCTCATAAAAC	GATGTTGGTCTTCCCTGTCC
KIF3a promoter	AAATCCCACTCTGTGCCAG	CTACCTGACCTCGCTTGATTG
KIF3a promoter-NC	CTCCTAACCTCAAGTGTTCCTC	GAATTTGCAACAGGGTGTGG
BBS4 promoter	CAGACAGGTAATGGAGAACGC	AATCGGCCATGGGATAAAGAG
BBS4 promoter-NC	AACACTTTGGGAGGTCAAGG	GTTTTGCCATATTGCCCAGG

Gating strategy of FACS



Tube: _001

Population	#Events	%Parent	%Total
All Events	30,000	####	100.0
P1	22,753	75.8	75.8
P2	19,967	87.8	66.6
P3	19,778	99.1	65.9

Supplementary Data 1. The potential MIF target genes related to cilia biogenesis identified with ChIP-seq.

Supplementary Data 2. The potential MIF target genes other than those related to cilia biogenesis.

Supplementary Data 3. The potential MIF binding proteins identified by protein chip analysis.

Supplementary Data 4. The potential MIF binding proteins identified by immunoprecipitation and mass spectrometry (MS) analysis in RCTE cells.